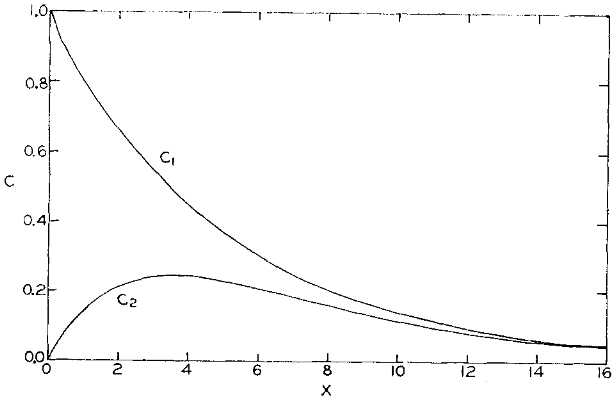

Fig. 1. Average concentration as a function of axial position.

$$\sum_i a_i \lambda_i^2 e^{-\lambda_i^2 x} J_o(\lambda_i) \qquad (9)$$

where the prime indicates differentiation. The solution to (9) is the sum of the solution to the homogeneous equation and the particular solution, or

$$b_j(x) = d_j e^{\frac{-\mu_j^2 x}{\alpha}} + \frac{2\beta K_1 J_1(\mu_j)}{K_2[J_o^2(\mu_j) + J_1^2(\mu_j)]} \sum_i a_i \lambda_i^2 J_o(\lambda_i) \frac{e^{-\lambda_i^2 x}}{\left(\frac{\mu_j^2}{\alpha} - \lambda_i^2\right)} \qquad (10)$$

where d_j are constants to be determined. The boundary condition at $x = 0$ is

$$\gamma = \frac{K_1}{K_2}\beta + \sum_j b_j(0) J_o(\mu_j y) \qquad (11)$$

The constants d_j are found by multiplying (11) by $y J_o(\mu_j y) dy$ and by integrating from 0 to 1. With the d_j determined, the $b_j(x)$ are known from (10) and the solution is seen to be

$$C_2 = \frac{K_1}{K_2}\beta \sum_j a_j J_o(\lambda_j) e^{-\lambda_j^2 x} + \sum_j \frac{2 J_o(\mu_j y) J_1(\mu_j)}{\mu_j [J_o^2(\mu_j) + J_1^2(\mu_j)]} \cdot \left\{ \left(\gamma - \frac{K_1}{K_2}\beta\right) e^{\frac{-\mu_j^2 x}{\alpha}} + \frac{K_1}{K_2}\beta \sum_i \frac{a_i \lambda_i^2 J_o(\lambda_i)}{\left[\frac{\mu_j^2}{\alpha} - \lambda_i^2\right]} \left(e^{-\lambda_i^2 x} - e^{-\mu_j^2 x/\alpha} \right) \right\} \qquad (12)$$

The average concentration in the tube as a function of axial position is

$$\overline{C}_n(x) = 2\int_0^1 y\, C(y, x) dy \quad n = 1, 2$$

These averages are shown in Figure 1 for $K_1 = 0.1$, $K_2 = 0.2$, $\gamma = 0$, $\beta = 1$, and a diffusivity ratio $\alpha = 0.5$. As is expected, the concentration of component 2 reaches a maximum before falling to zero.

NOTATION

c_n = concentration, $n = 1, 2$
c_{no} = inlet concentration
C_n = c_n/c_{10}
D_n = diffusivity
k_n = reaction rate constant
K_n = $k_n R/D_1$
r = radial position
R = tube radius
V = fluid velocity
x = $D_1 z/R^2 V$
y = r/R
z = axial position

Greek Letters

α = D_1/D_2
β = stoichiometric coefficient
γ = c_{20}/c_{10}
λ_i, μ_j = eigenvalues
η defined by Equation (5)

LITERATURE CITED

1. Baron, Thomas, W. R. Manning, and H. F. Johnstone, *Chem. Eng. Progr.*, **48**, 125 (1952).
2. Katz, S., *Chem. Eng. Sci.*, **10**, 202 (1959).
3. Wissler, E. H., and R. S. Schechter, *App. Sci. Res.*, **A10**, 198 (1961).

Predicting Vertical Film Flow Characteristics in the Entrance Region

DUANE F. BRULEY

Clemson University, Clemson, South Carolina

Liquid films flowing over vertical surfaces under the influence of gravity are encountered in many types of heat and mass transfer equipment: distillation columns, evaporators, wetted wall columns. Therefore, a complete understanding of film flow, from the entrance to the exit, should be of interest industrially, experimentally, and academically.

Many papers concerning film flow have been published since the early 1900's. However, there is still much to be learned before precise design calculations can be carried out for operations involving this flow phenomenon. Dunkler and Bergelin (2) discussed the importance of understanding the mechanics of film flow to the analysis of performance of industrial equipment. The authors pointed out that it is necessary to know the exact area for mass or heat transfer so that a combined coefficient *ka* is not required for design purposes. The mass transfer coefficient *k* and the area for transfer *a* are independent functions and should be treated as such if a rational analysis is to be made.

Although many experimental methods (*1, 3, 4, 6*) have been used to determine film thicknesses, most of the investigations have been done in the

INFORMATION RETRIEVAL

(*Continued from page 944*)

Freezing front motion and heat transfer outside an infinite, isothermal cylinder, Tien, L. C., and S. W. Churchill, **A.I.Ch.E. Journal, 11,** No. 5, p. 790 (September, 1965).

Key Words: A. Calculation-8, Temperature-9, Freezing-8, Cylinder-9, Outside-9, Isothermal-0, Heat Transfer-8, Computer-10. B. Freezing-8, Outside-9, Soil-9, Pipes-9, Tanks-9, Storage-10, Underground-0.

Abstract: A numerical method is developed for calculation of the temperature field in a material that freezes outside an isothermal cylinder. Numerical values are presented for the freezing front location and for the rate of heat transfer to the cylinder. The computed values are compared with the analytical solutions for the limiting cases of zero latent heat, negligible heat capacity, and freezing adjacent to a flat plate. The results have many applications, including the freezing of wet soil outside underground pipes or storage tanks for cryogenic fluids.

Measurement of the void fraction in two-phase flow by x-ray attenuation, Pike, R. W., Bert Wilkins, Jr., and H. C. Ward, **A.I.Ch.E. Journal, 11,** No. 5, p. 794 (September, 1965).

Key Words: A. Measurement-8, Void Fraction-9, 8, Two-Phase Flow-9, Steam-5, Water-5, X-Ray Attenuation-10, Flow Patterns-9.

Abstract: The use of an x-ray tube was shown to be an effective source of monoenergetic radiation for the measurement of the void fraction in two-phase, steam-water flow with the proper selection of the tube wall thickness, x-ray tube operating conditions, collimation, and traverse time. Equations for the local and average void fraction and the statistical error were confirmed applicable by the mock-up technique. This consisted of simulating the two-phase, steam-water flow patterns with mock-ups of Lucite and air. Experimental data show that confidence could be placed in the measurements to within the probable statistical error, as all deviations were less than the probable error. Measured local and average void fractions for steam-water, two-phase flow are given.

The condensation of mixed vapors, Estrin, Joseph, T. W. Hayes, and T. B. Drew, **A.I.Ch.E. Journal, 11,** No. 5, p. 800 (September, 1965).

Key Words: A. Condensation-8, Mass Transfer-8, 9, Mass Transfer Coefficient-8, 7, Heat Transfer Coefficient-8, Molecular Weight-6, Drew-Colburn Coefficient-7, 8, Rate-6, Forced Convection-10, Ethanol-1, Alcohol-1, Water-1, Experimental-0.

Abstract: This work describes the condensation process in which two condensable components are involved, and the mass transfer process consequently involves their partial fractionation. The effect of molecular weight difference of the diffusing components upon the mass transfer coefficient was studied. The experimental results indicate that the value of the Drew-Colburn coefficient is affected by molecular weight differences of the components as explained by the theory.

(*Continued on page 948*)

terminal flow region. The work of Wilkes and Nedderman (*11*), however, considered the entrance region both theoretically and experimentally. In their analysis the liquid flowed through a complicated distributing device at the top of the column which formed a parabolic velocity profile in the liquid phase at the entrance to the wetted section. In the entrance region the velocity profile was found to change from full parabolic to half parabolic.

The problem considered here is free flow over the leading edge of a vertical surface. A mathematical model consisting of the two-dimensional boundary-layer and continuity equations was formulated and solved numerically to predict entrance region lengths, film thicknesses and velocity profiles. The laminar flow boundary-layer model was chosen, since the Nusselt equations are considered valid over the Reynolds number range of interest, 0 to 1,500 (*8*). Also, observations (*10, 11*) that flow in the entrance region is smooth and undisturbed, as compared with terminal flow at the same Reynolds numbers, supports the laminar flow model assumption.

MATHEMATICAL FORMULATION

Figure 1 illustrates the assumed entrance region flow scheme for the steady, isothermal, laminar flow of an incompressible Newtonian fluid over the leading edge of a vertical plate. The coordinate system was chosen such that the plate is parallel to the x-z plane and the film thickness is measured in the y direction.

Considering the flow to be independent of the z direction, one can express the two-dimensional boundary-layer and continuity equations as follows.

$$u\frac{\partial u}{\partial x} + v\frac{\partial u}{\partial y} = g + \nu\frac{\partial^2 u}{\partial y^2} \tag{1}$$

$$\frac{\partial u}{\partial x} + \frac{\partial v}{\partial y} = 0$$

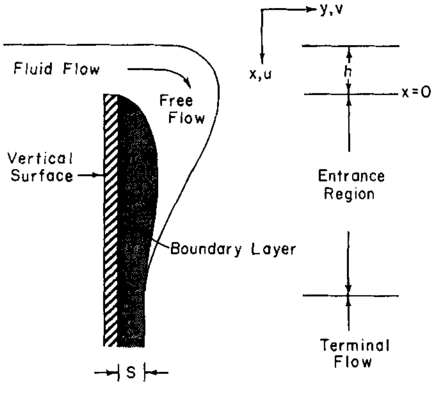

Fig. 1. Entrance-region flow scheme.

With the no-slip condition assumed at the solid surface, the boundary layer begins to form immediately. Due to the asymptotic approach to the free stream velocity the boundary layer was defined (*9*) to be the thickness at which the vertical velocity u reached 99% of the free stream velocity $\bar{u}_\infty$. The problem is complicated by the fact that the free stream velocity is not constant, but is a function of vertical position due to gravitational acceleration. The following equation was used to calculate the free stream velocity:

$$\bar{u}_\infty = \sqrt{\bar{u}_o^2 + 2gx} \tag{2}$$

This, of course, assumes that the fluid outside the defined boundary layer is in frictionless free fall and that thus negligible forces exist at the air-water interface.

Choosing $x = 0$ and $y = 0$ at the leading edge of the plate results in the following boundary conditions.

$$\begin{array}{lll} u = \bar{u}_0 \quad v = 0 & \text{at} & x = 0 \\ u = v = 0 & \text{at} & y = 0 \\ u = 0.99\,\bar{u}_\infty & \text{at} & y = \beta \end{array} \tag{3}$$

The model assumes that the vertical velocity at the leading edge is uniform and can be approximated by the following free-fall equation.

$$\bar{u}_0 = \sqrt{2gh} \tag{4}$$

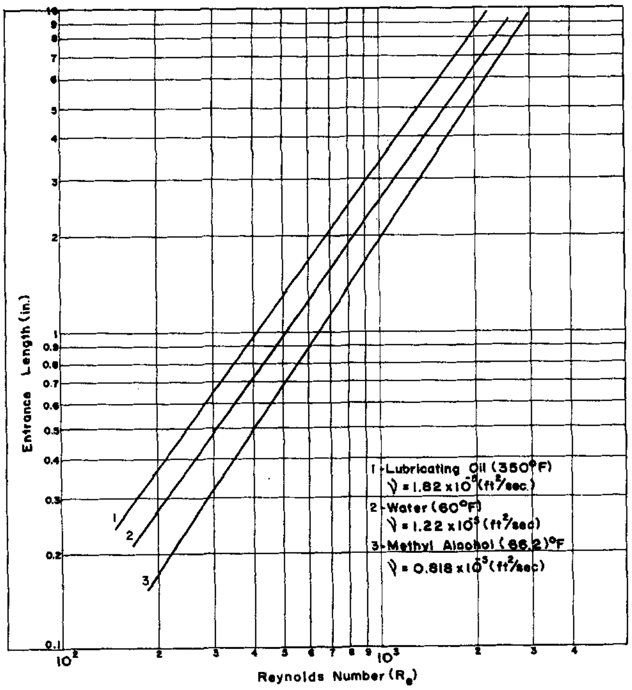

Fig. 2. Predicted entrance lengths as a function of Reynolds number and kinematic viscosity.

The Francis Weir equation (*7*) was used to estimate the distance h of the fluid standing above the leading edge.

$$h = \sqrt[2/3]{\frac{Q}{3.33}} \tag{5}$$

The equations and boundary conditions were converted to finite difference form and solved numerically on a digital computer with a "marching ahead" calculation similar to the method used by Wu (*12*) for horizontal flat plates. The differenced equations are

$$u_{m+1,n} = u_{m,n} + A\left[\frac{u_{m,n+1}}{u_{m,n}} + \frac{u_{m,n-1}}{u_{m,n}} - 2\right] + B\left[\frac{v_{m,n}\,u_{m,n-1}}{u_{m,n}} - \frac{v_{m,n}\,u_{m,n+1}}{u_{m,n}}\right] + \frac{C}{u_{m,n}} \tag{6}$$

$$v_{m+1,n} = v_{m+1,n-1} - D(u_{m+1,n-1} - u_{m,n-1} + u_{m+1,n} - u_{m,n}) \tag{7}$$

where

$$A = \frac{\nu\Delta x}{\Delta y^2} \quad B = \frac{\Delta x}{2\Delta y}$$
$$C = g\Delta x \quad D = \frac{\Delta y}{2\Delta x} \tag{8}$$

and the boundary conditions in differenced form are

$$\begin{array}{l} u_{m,o} = v_{m,o} = v_{o,n} = 0 \\ u_{o,n} = \bar{u}_o \\ u_{m,\beta} = 0.99\,\bar{u}_\infty \end{array} \tag{9}$$

where

$$\bar{u}_\infty = \sqrt{\bar{u}_o^2 + 2gm\Delta x} \tag{10}$$

The mass flow rate of fluid in the boundary layer at any vertical position m was estimated with the following equation.

$$FB = \rho L\Delta y \sum_{n=0}^{\beta} \frac{(u_{m,n} + u_{m,n+1})}{2} \tag{11}$$

All the remaining fluid was considered to be flowing outside the boundary layer in free fall at a velocity $\bar{u}_\infty$, so that

$$F0 = \rho L z \bar{u}_\infty \tag{12}$$

Therefore, for any given case where the total flow rate F was known it was possible to calculate z.

$$z = \frac{F - FB}{\rho L \bar{u}_\infty} \tag{13}$$

The total film thickness was then predicted as the sum of the boundary-layer thickness and z.

To allow for continued flow development after all the fluid is in the boundary layer another condition was imposed. At this point all the fluid feels the viscous forces created by the solid boundary at the plate. Since no fluid is in free fall the condition that FB [Equation (11)] must equal the total flow F was enforced. The entrance length was then defined as the distance from the leading edge at which the surface velocity reached 99.99% of its asymptotic value (terminal flow surface velocity).

NUMERICAL SOLUTION

The mathematical model was solved numerically to eliminate idealizations necessary in obtaining an analytical solution. Although this approach appears straightforward several mathematical difficulties had to be resolved before a stable, converging solution could be obtained. For instance, an average difference approximation for $\partial u/\partial x$ in the momentum equation leads to instability, while a forward difference approximation does not (*13*).

Stability conditions were determined by the method of Karplus (*5*) to give first approximations for Δx values based on suitably sized Δy's. Stability and convergence characteristics were then tested by varying the increment

INFORMATION RETRIEVAL

(Continued from page 946)

Mixing effects in a spray-column heat exchanger, Letan, Ruth, and Ephraim Kehat, **A.I.Ch.E. Journal, 11,** No. 5, p. 804 (September, 1965).

Key Words: A. Temperature Profiles-8, Heat Exchanger-9, Spray Column-9, Kerosene-5, Water-5, Mixing-6, Temperature-7, Holdup-6, Flow Rate-6, Heat Transfer-8, 9, Physical Model-8.

Abstract: Temperature profiles were measured in a spray-column heat exchanger between the inlets of warm kerosene and cold water. The temperature jump at the inlet of the continuous phase is a measure of the amount of mixing in the column and is a function of holdup and ratio of flow rates of the two phases. A physical model for heat transfer in a spray column based on hydrodynamic principles is proposed. The physical model is applied to explain the data on temperature jumps in spray-column heat exchangers and data on concentration jumps in spray-column extractors.

Heat transfer to decomposing nitrogen dioxide in a turbulent boundary layer, Brian, P. L. T., R. C. Reid, and S. W. Bodman, **A.I.Ch.E. Journal, 11,** No. 5, p. 809 (September, 1965).

Key Words: A. Gas-5, Nitrogen-5, Nitrogen Dioxide-5, Reaction Rate-6, Temperature-6, Pressure-6, Speed-6, Rotation-9, Diffusion-8, Heat Transfer-8, 7, Mass Transfer-8, 7, Eddy Diffusion-8, Turbulent Flow-9, Cylinder-10, Heat-10.

Abstract: Heat transfer coefficients were measured for the dissociating system $2\,NO_2 \leftrightarrows 2NO + O_2$ in turbulent flow. Heat transfer rates to this reacting gas are limited by the kinetics of the decomposition and recombination reactions. Experimental results agree to within 10% with a film-theory solution for heat transfer accompanied by a nonequilibrium chemical reaction.

Motion of gas bubbles in non-Newtonian liquids, Astarita, Gianni, and Gennaro Apuzzo, **A.I.Ch.E. Journal, 11,** No. 5, p. 815 (September, 1965).

Key Words: A. Motion-8, Gas Bubbles-9, Liquids-9, Fluids-9, Non-Newtonian-0, Viscous-0, Viscoelastic-0, Flow-8, Power Law-10, Stokes Regime-9, Hadamard Regime-9, Levich Regime-9, Taylor Regime-9, Volume-8, Velocity-8, Shape-8.

Abstract: The available theoretical knowledge on the motion of gas bubbles in Newtonian liquids is reviewed, and the possibility of extension to non-Newtonian liquids, both purely viscous and viscoelastic, is studied. Experimental data on the rising velocities of gas bubbles in a variety of non-Newtonian liquids are presented and interpreted on the basis of theoretical knowledge. Peculiarities which have been observed in highly elastic liquids are discussed, and a tentative interpretation is offered.

Ion flotation of dichromate with a cationic surfactant, Grieves, Robert B., Thomas E. Wilson, and Kenneth Y. Shih, **A.I.Ch.E. Journal, 11,** No. 5, p. 820 (September, 1965).

Key Words: A. Potassium Dichromate-1, Ethylhexadecyldimethylammonium Bromide-1, Foam-2, 5, Dichromate Mixture-2, Surfactant Mixture-2, Gas Bubbles-4, Water-5, Dichromate-9, Mass-6, Surfactant-9, Concentration-6, 7, 9, Hydrogen Ion-9, Interfering Anion-9, Residual-0, Volume-7, Foam-9, Enrichment Ratio-7, Removal Ratios-7, Foam Separation-8, Ion Flotation-8, Mass Transfer-8, Removal-9, Foaming-10, Aeration-10.

Abstract: An experimental investigation is presented of the flotation of dichromate ion from aqueous solution with a cationic surfactant, ethylhexdecyldimethylammonium bromide. Dichromate forms a colloidal complex with EHDA ion in a molar ratio of approximately 1:2. Excess surfactant brings about the formation of a stable foam to which the complex is adsorbed, providing the separation of dichromate from aqueous solution. Batch flotation studies were conducted utilizing approximately 2 liter solutions containing from 10 to 200 mg. of dichromate ion, with masses of EHDA-Br ranging from 400 to 800 mg. The effects of mass of surfactant added, dichromate concentration, *p*H, and possible interfering anions were determined. A comparison is made with pure surfactant solutions, and the mechanism of the process is discussed.

(Continued on page 950)

---

sizes around the predicted values and checking the solutions on the computer.

The numerical calculation was started using the boundary conditions at $m = 0$ and solving the equation of motion (6) for values of $u_{1,n}$ until $u_{1,n} = 0.99\ \bar{u}_\infty$. Values for $v_{1,n}$ were then determined by solving the continuity equation (7). This procedure was repeated over and over, each time "marching ahead" one increment in m until Equation (11) indicated that all the fluid was flowing in the boundary layer ($FB = F$). At this point Equation (11) was used as a boundary condition during further flow development until the model surface velocity reached 99.99% of the terminal flow surface velocity.

RESULTS

Three liquids were studied over a Reynolds number range of 262.8 to 1,493. The fluids were water, methyl alcohol, and SAE10 lubricating oil (21°API) with kinematic viscosities as follows

Methyl alcohol (66.2°F.)
$\nu = 0.818 \times 10^{-5}$ (sq.ft./sec.)
Water (60°F.)
$\nu = 1.22 \times 10^{-5}$ (sq.ft./sec.)
Lubricating oil (350°F.)
$\nu = 1.82 \times 10^{-5}$ (sq.ft./sec.)

Eleven cases were calculated with the numerical step-by-step solution of the two-dimensional boundary-layer and continuity equations. Entrance lengths were predicted at different flow rates and plotted against Reynolds number on logarithmic paper. As can be seen in Figure 2 the plots are essentially straight parallel lines which obey the following formula.

$$(EL) = a(Re)^b \qquad (14)$$

For the fluids examined the constants were found to be

Methyl alcohol (66.2°F.)
$a = 5.87 \times 10^{-5}$ $b = 1.5079$
Lubricating oil (350°F.)
$a = 3.14 \times 10^{-4}$ $b = 1.3420$
Water (60°F.)
$a = 2.013 \times 10^{-4}$ $b = 1.3695$

It is interesting to note that for equal Reynolds numbers $\left(Re = \dfrac{4Q}{\nu}\right)$ the entrance lengths are longer for the more viscous fluids. This, of course, is true because of the proportionately larger volumetric flow rate. For equal volumetric flow rates the entrance length is less for the more viscous fluids.

Figure 3 compares the predicted film profiles and entrance lengths for

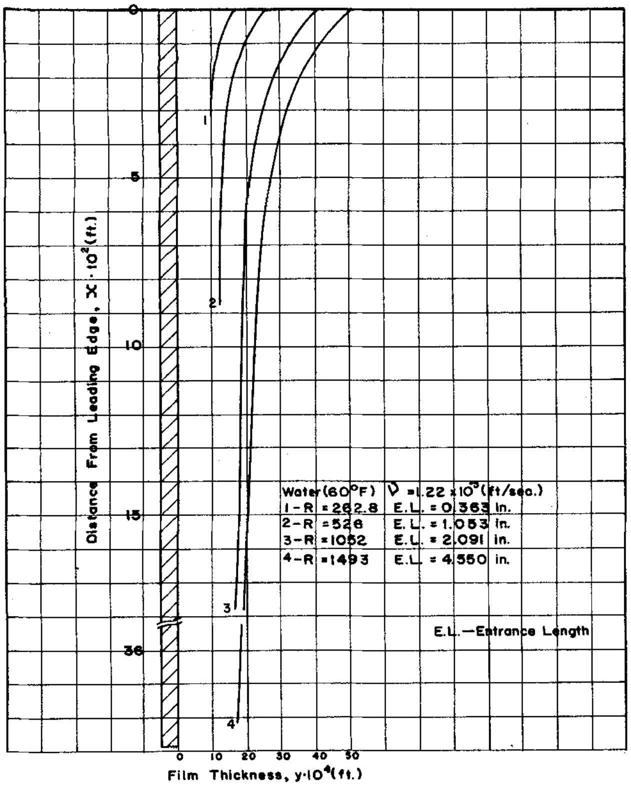

Fig. 3. Predicted profiles and entrance lengths.

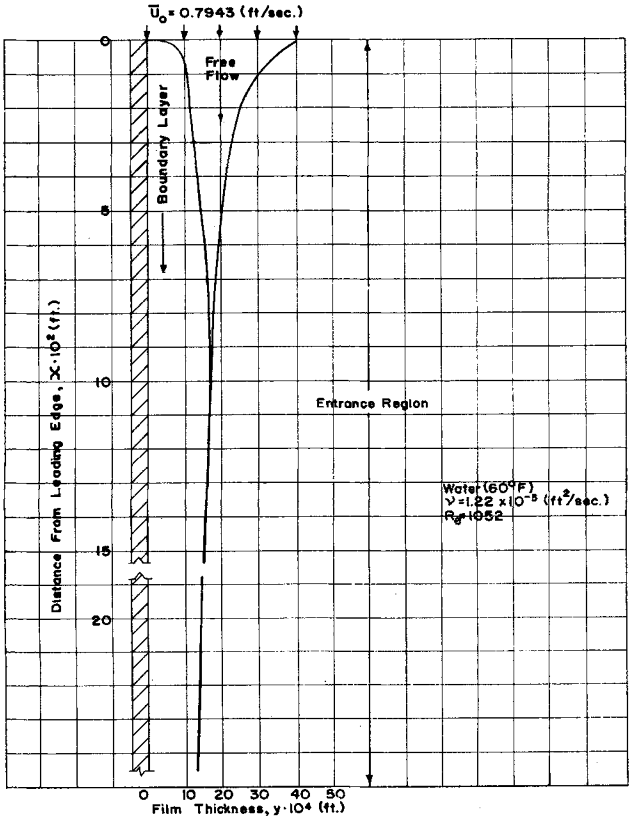

Fig. 4. Flow pattern predicted by the boundary-layer equations.

water at different Reynolds numbers. The curves show that at the lowest Reynolds number $Re = 262.8$ the entrance effects are essentially negligible, but as the Reynolds number is increased they become more and more significant. For example the terminal film thickness is only 1.8 times as great for $Re = 1{,}493$ as compared with the case where $Re = 262.8$. However, the entrance length is about 12.3 times as long and the initial film thickness is about 3.13 times as thick for the $Re = 1{,}493$ case as compared with the $Re = 262.8$ case.

Figure 4 illustrates in more detail the entrance region for the case of water at a Reynolds number of 1,052. The appearance of a sharp boundary-layer buildup at the leading edge is exaggerated by the relative ordinate and abscissa scales. If equal scales had been used the buildup would have appeared much more gradual. It is also obvious that most of the flow development takes place before all the free-fall fluid is included in the boundary layer. Therefore, the effective entrance region might be considered somewhat shorter than that presented here.

For all the cases considered here the numerically calculated point velocities and film thicknesses checked within 4% of those determined with the standard terminal flow equations.

$$s = \sqrt[3]{\frac{3\nu Q}{g}}$$

$$U_s = \frac{gs^2}{2\nu}$$

The accuracy could have been increased by decreasing the increment sizes but the already lengthy computation time made this impractical.

ACKNOWLEDGMENT

The author is grateful to the Clemson University Engineering Research Station for the financial support of this work. Also many thanks are given to M. C. Palmer and his Computing Center staff for their invaluable assistance in writing the needed machine language program.

NOTATION

A = constant in differenced equations
a = constant in entrance length empirical equation
B = constant in differenced equations
b = constant in entrance length empirical equation
C = constant in differenced equations
D = constant in differenced equations
EL = entrance length, ft.

INFORMATION RETRIEVAL

(Continued from page 948)

Heat transfer in a fuel cell battery, Gidaspow, Dimitri, and Bernard S. Baker, **A.I.Ch.E. Journal, 11,** No. 5, p. 825 (September, 1965).

Key Words: A. Heat Transfer-8, Conduction-8, Convection-8, Fuel Cell-9, Battery-9, Thermal Buckling-8, Temperature-8.

Abstract: Analytical solutions were obtained for temperature distributions in a single adiabatic fuel cell. With these results it is possible to characterize heat transfer in a battery with convection in the fuel and air streams, and with conduction of heat in three directions, by means of an average temperature for which an analytical solution was also obtained. Although the temperature can be kept within safe limits in low power density batteries, the paper shows that critical dimensions exist beyond which failure by thermal buckling will occur.

Scale-up for viscoelastic fluids, Slattery, John C., **A.I.Ch.E. Journal, 11,** No. 5, p. 831 (September, 1965).

Key Words: A. Scale-Up-8, Process-9, Fluid-1, Viscoelastic-0, Noll's Theory-10, Turbulent-0, Flow-9, Pipe-9, Non-Newtonian-0, Pressure Drop-9, Flow Rate-9.

Abstract: A suggestion is made as to how one might proceed to scale up a process involving an arbitrary viscoelastic fluid. The discussion is based upon Noll's theory of simple fluids. Turbulent flow in an infinitely long pipe is taken as an illustration.

Mass transfer at high mass fluxes: Part I. Evaporation at the stagnation point of a cylinder, Mendelson, Harvey, and Stephen Yerazunis, **A.I.Ch.E. Journal, 11,** No. 5, p. 834 (September, 1965).

Key Words: A. Mass Transfer-8, Water-1, Liquid-1, Carbon Tetrachloride-1, Vapor-2, Evaporation-8, 7, Temperature-6, Geometry-6, Cylinder-9, 10, Reynolds Number-6, Schmidt Number-6, Stagnation Point-6, Evaporation Rate-7, Evaporation Coefficient-6, Wind Tunnel-10.

Abstract: An experimental method for measuring mass transfer rates at high mass fluxes is developed for the case of evaporation at the stagnation point of a cylinder. Evaporation of carbon tetrachloride at the stagnation point was measured and determined to be consistent with theoretical predictions. It was observed that water exhibits a significant interfacial resistance to evaporation at high transfer rates. Evaporation coefficients based on the discrepancy between experimental determinations and theoretical expectations were found to be a strong function of temperature and to be consistent with the majority of reported measurements made at lower temperatures. The experimental method should be useful for application to other configurations and flow conditions for studying mass transfer at high mass fluxes.

Performance of a packed distillation column with electrically heated packing, Somer, Tarik G., **A.I.Ch.E. Journal, 11,** No. 5, p. 840 (September, 1965).

Key Words: A. Performance-8, 7, Efficiency-8, 7, Packed Column-9, 8, Heating-8, 6, Electricity-10, Packing-9, Carbon Tetrachloride-2, Benzene-2, Transfer Units-7, Mass Transfer-7, Aromatic Hydrocarbons-2, Coke-5.

Abstract: Electric current was applied across the coke packing of a glass column, distilling carbon tetrachloride-benzene at total reflux. Heat generated by electricity boiled the liquid on the packing surface. Bubbles rising across the liquid film reduced its resistance to mass transfer, improving the column efficiency. Theoretical analysis and experimental results are presented.

(Continued on page 952)

F = mass flow rate, lb.$_m$/ft.-sec.
FB = mass flow rate in the boundary layer, lb.$_m$/(ft.)(sec.)
FO = mass flow rate in free fall, lb.$_m$/(ft.)(sec.)
g = acceleration of gravity—32.2, ft./sec.^{2}
H = head of fluid above vertical plate, ft.
L = unit length, ft.
Q = volumetric flow rate, cu.ft./(sec.)(ft.)
Re = Reynolds number, $(4Q/\nu)$
s = terminal film thickness, ft.
u = velocity in the x direction ft./sec.
u_s = terminal surface velocity, ft./sec.
$\overline{u_c}$ = liquid velocity at leading edge, ft./sec.
$\overline{u_x}$ = variable free stream velocity, ft./sec.
v = velocity in the y direction, ft./sec.
x = entrance length cartesian coordinate, ft.
y = film thickness cartesian coordinate, ft.
Z = plate length cartesian coordinate, ∞
z = free stream thickness, ft.

β = numerically calculated boundary-layer thickness, ft.
Δ = finite increment
ν = kinematic viscosity, sq.ft./sec.
ρ = density, lb.$_m$/cu.ft.

Subscripts

m = x direction
n = y direction

LITERATURE CITED

1. Cooper, C. M., T. B. Drew, and W. H. McAdams, *Trans. Am. Inst. Chem. Engrs.*, **30** 158 (1934).
2. Dukler, A. E., and P. O. Bergelin, *Chem. Eng. Progr.*, **48**, 557 (1952).
3. Fallah, R., T. G. Hunter, and A. W. Nash, *J. Soc. Chem. Ind.*, **53**, 369T (1934).
4. Jackson, M. L., *A.I.Ch.E. J.*, **1**, 231 (1955).
5. Karplus, W. J., *Trans. AIEE*, **77**, 1 (1958).
6. Kirkbride, C. G., *Trans. Am. Inst. Chem. Engrs.*, **30**, 170 (1934).
7. Perry, J. H., "Chemical Engineering Handbook," 3 ed., p. 601, McGraw-Hill, New York (1950).
8. Portalski, S., *Chem. Eng. Sci.*, **18**, 787 (1963).
9. Schlichting, H., "Boundary Layer Theory," 4 ed., p. 168, McGraw-Hill, New York (1960).
10. Wendel, M. M., and R. L. Pigford, *A.I.Ch.E. J.*, **4**, 249 (1958).
11. Wilkes, J. O., and R. M. Nedderman, *Chem. Eng. Sci.*, **17**, 177 (1962).
12. Wu, J. C., *Proc. 1961 Heat Transfer and Fluid Mech. Inst.*, 55-69 (1961).